

## Roles of the Brazilian Plateau in the Formation of the SACZ

YASU-MASA KODAMA,\* TOMOYUKI SAGAWA, AND SACHINOBU ISHIDA

*Graduate School of Science and Technology, Hirosaki University, Hirosaki, Aomori, Japan*

TAKAO YOSHIKANE

*Research Institute for Global Change, Japan Agency for Marine-Earth Science and Technology, Yokohama, Kanagawa, Japan*

(Manuscript received 13 April 2010, in final form 12 October 2011)

### ABSTRACT

The role of the Brazilian Plateau (BP) in maintaining the South Atlantic convergence zone (SACZ) has been examined by statistical analysis and numerical experiments. Statistical analysis using 27 years of data showed that the SACZ is most intense when it is over the BP. In this case, low-level cyclonic circulation appears over the southwestern part of the BP and forms westerly flow, which intensifies low-level convergence along the SACZ with northeasterly flow from the Amazon and northerly flow along the western edge of the South Atlantic subtropical high. A vorticity budget analysis indicates that precipitation over the BP that accompanies stretching maintains the cyclonic circulation.

Sensitivity experiments using a regional atmospheric model for two different cases indicate that precipitation over the BP plays a dominant role as an atmospheric heat source in maintaining the cyclonic circulation and the SACZ. In model experiments in which rain was stopped around the BP but the topography was kept, the cyclonic circulation disappeared, and the SACZ shifted southward away from its original position. In comparison with a control run, precipitation over the BP was weakened and the SACZ shifted southward in experiments in which the BP was removed or its complex, multiple-valley terrain was smoothed out. The results of this study support the ideas suggested in previous studies (i.e., that the BP has an anchor effect on the SACZ): Precipitation is intensified over the complex terrain of the BP, and mechanisms of conditional instability of the second kind occur between the precipitation over the BP and the cyclonic circulation to its southwest, which intensifies moisture convergence over the plateau.

### 1. Introduction

The South Atlantic convergence zone (SACZ) is a pre-dominant precipitation zone extending from the Amazon basin to the South Atlantic, passing through the southeastern part of South America. The SACZ develops in austral summer and is an important component of the South American summer monsoon (SASM) (Zhou and Lau 1998; Kodama 1992, 1993; Figueroa et al. 1995; Carvalho et al. 2004; Vera et al. 2006). The SACZ is one of the significant subtropical convergence zones (STCZs)

(Kodama 1993; Ninomiya 2007), which also include the baiu frontal zone (BFZ) over East Asia and the western North Pacific, which develops in early boreal summer, and the South Pacific convergence zone (SPCZ), which develops in austral summer over the South Pacific. Other weaker STCZs appear over the southern Indian Ocean and the western North Atlantic (Kodama 1993; Cook 2000; Ninomiya 2008). Significant STCZs are climatically developed where low-level poleward flow toward the subtropical latitudes (30°N or 30°S) along the western periphery of the subtropical high is strong and subtropical jets flow in the subtropical latitudes in summer. Weaker poleward wind over the southern Indian Ocean and the location of the subtropical jet out of the subtropical latitude in summer over the western North Atlantic cause weaker STCZs in these areas (Kodama 1993).

Seasonal changes in the climatological position of the SACZ are small between austral spring and summer (Diaz and Aceituno 2003). This is in contrast to the

---

\* Current affiliation: Seiai Junior and Senior High School, Hirosaki, Aomori, Japan.

---

*Corresponding author address:* Yasu-Masa Kodama, Graduate School of Science and Technology, Hirosaki University, Hirosaki, Aomori, 036-8561, Japan.  
E-mail: kodama@cc.hirosaki-u.ac.jp

BFZ, which migrates northward from 25° to 40°N with a seasonal march between June and August (Ding 1992), and to the SPCZ, which shifts in an east–west direction in accordance with the El Niño–Southern Oscillation (ENSO) (Murakami et al. 1986; Streten 1975; Kodama 1993). The SACZ shifts in a northeast–southwest direction while keeping a southeastward orientation toward the South Atlantic around a position extending over the Brazilian Plateau (BP). It shows seesaw or dipole variations with a similar precipitation zone over southern Brazil, Uruguay, and Argentina on intraseasonal and interannual time scales (Nogues-Paegle and Mo 1997; Liebmann et al. 1999; Nogues-Paegle and Mo 2002; Carvalho et al. 2004; Grimm and Zilli 2009). The intraseasonal variation in continental and oceanic portions is not connected (Muza et al. 2009). Moisture sources also differ between the portions (Muza et al. 2009; Carvalho et al. 2010), being northerly from the equatorial Atlantic and northeasterly from the Amazon for the continental portion, and northerly from eastern South America and from over the Atlantic for the oceanic portion. Wave trains in the Pacific–South America pattern contribute to maintaining the intraseasonal variation of the oceanic portion.

In this paper, we will show that the SACZ is most intense when it extends just over the BP. This suggests a strong influence of the BP on the SACZ. The BP includes several peaks above 2500 m, but most of the plateau is not high (~1000 m). It has a wide extent, with complex terrain and many narrow valleys. The BP, which is located near the southeastern coast of South America, has both topographic and coastal effects on the SACZ. Before Grimm et al. (2007), studies on mechanisms of the SACZ paid little attention to the contribution of the BP. Numerical experiments showed a large contribution of latent heating over the Amazon basin (Figueroa et al. 1995), along with latent heating along the SACZ (Kodama 1999), for maintaining the large-scale low-level and upper-level circulation around the SACZ. Lenters and Cook (1995) noted the strong dependence of precipitation on the behavior of the heat low over the continent related to a continent–ocean thermal contrast. Previous perspectives on conditions and factors influencing the SACZ, along with the South American summer monsoon, have been summarized by Grimm et al. (2005) and Vera et al. (2006).

Grimm et al. (2007) first suggested a contribution of the BP to the SACZ. They found a negative correlation between precipitation over the BP in austral spring and precipitation over central-eastern Brazil in the following summer by analyzing 41-yr surface observation data. They reported that lower soil moisture over the BP in spring produces higher air temperature near the

surface over the plateau. This situation can be a trigger for stronger precipitation over the SACZ in summer since higher air temperature produces anomalous convergence over the BP and cyclonic circulation that increases moisture flux from northern and central South America into central-eastern Brazil and enhances precipitation. This effect is also associated with the topographic effect of the BP and would not happen in the absence of the topographic features in the region. After precipitation is enhanced, near-surface air temperature decreases but the tropospheric heating by precipitation still maintains and intensifies convergence and cyclonic circulation over southeast Brazil (southwest of the BP) for a while, thanks to the conditional instability of the second kind (CISK) mechanism.

To confirm this hypothesis, Grimm et al. (2007) performed a sensitivity experiment for one case using a regional climate model with a 60-km horizontal resolution. They found that lower soil moisture in spring around the BP intensifies the cyclonic circulation. They also found that removal of the BP from the model weakens the cyclonic circulation in the original position and shifts the SACZ southward. Grimm and Zilli (2009) examined the relationship between the dipole (seesaw) of the SACZ and the cyclonic circulation in the southeast of Brazil. They revealed that negative height (cyclonic) anomalies induce a strong rainfall anomaly around the BP and maintain the continental portion of the SACZ, whereas positive height (anticyclonic) anomalies induce a strong rainfall anomaly over southern Brazil, Uruguay, and Argentina. From these findings, Grimm et al. (2007) and Grimm and Zilli (2009) suggested that the BP anchors the dipole mode of precipitation over South America, with the northern peak of the dipole over the BP. This effect may be related to the low climatic migration of the SACZ compared to the BFZ and the SPCZ, which show large seasonal and interannual movement.

However, many problems remain unsolved. The numerical experiments by Grimm et al. (2007) were performed for only one case study, and the conclusions were not definitive, as the authors mentioned. Here we investigate two other case studies. Grimm et al. (2007) used 60-km resolution. However, considering the complex terrain of the BP, with many narrow valleys, 60 km may be inadequate. We used a 25-km-mesh model and examined the influence of the BP and model resolution in experiments with altered topography around the BP and different grid sizes. In these experiments, we examined how the representation of the BP in the model influenced the precipitation over South America. We also performed another sensitivity experiment in which precipitation around the BP was artificially stopped to examine the role of latent heat around the BP in maintaining the cyclonic circulation.

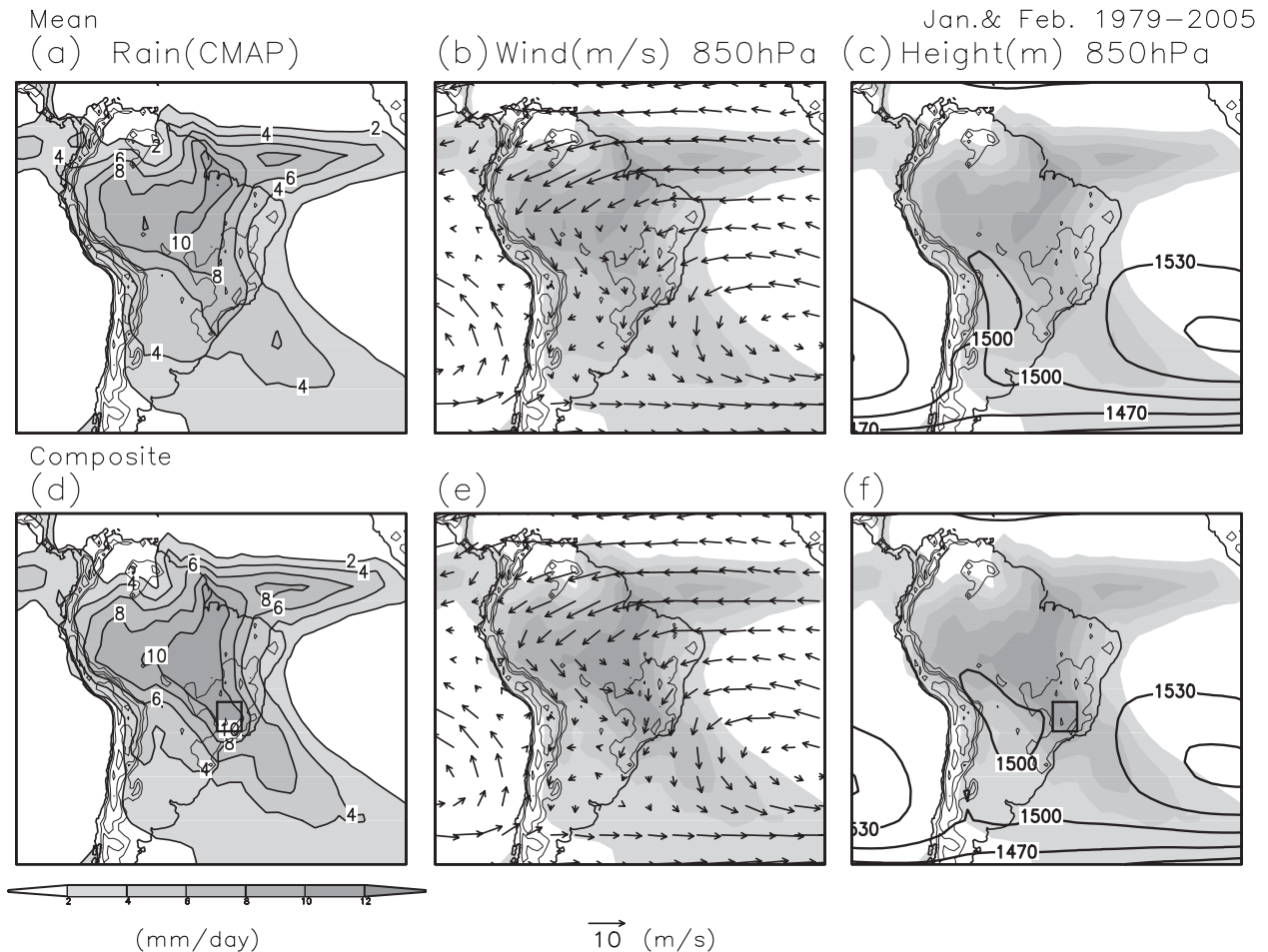


FIG. 1. Long-term (between 1979 and 2005) (a) averaged precipitation, (b) low-level (850 hPa) wind, and (c) geopotential height in austral summer (January and February). (d)–(f) As in (a)–(c), but showing composite fields for the selected 17 months when monthly averaged precipitation exceeded  $8 \text{ mm day}^{-1}$  over the reference area shown in a thick rectangle in (d) and (f). Precipitation is shown by shading and contours in (a) and (d) and by shading only in (b), (c), (e), and (f).

Our study aim was to examine the role of the BP in the formation of the SACZ, including its anchoring effect. In section 2, the data and model are described. Results of statistical studies and a vorticity budget analysis are described in section 3. The design of sensitivity experiments in the model simulation are described in section 4. The results of our numerical experiments are presented in section 5. A vorticity budget analysis of the results is described in section 6, and we summarize our results in section 7.

## 2. Data for analysis and models in the numerical experiments

Monthly averaged National Centers for Environmental Prediction–National Center for Atmospheric Research (NCEP–NCAR) reanalysis data for austral summers (January and February) were used in the statistical

analysis. Twenty-seven seasons between January 1979 and February 2005 were studied. Monthly averaged outgoing longwave radiation (OLR) (Liebmann and Smith 1996) and Climate Prediction Center (CPC) Merged Analysis of Precipitation (CMAP) (Xie and Arkin 1997) data were also used. We used the Tsukuba University, Japan, Terrestrial Environmental Research Center Regional Atmospheric Modeling System for numerical experiments (hereafter TERC-RAMS). The TERC-RAMS (Sato and Kimura 2003) is a modified version of the RAMS (Pielke et al. 1992) that was developed at TERC. A radiation scheme (Nakajima et al. 2000) and Arakawa–Shubert parameterization coded by Numaguti et al. (1997) are applied in the TERC-RAMS. The model resolution is 25 km over the domain around South America. Initial and boundary conditions were obtained from 6-hourly NCEP–NCAR reanalysis data with  $2.5^\circ \times 2.5^\circ$  (lat  $\times$  lon) resolution. Boundary conditions

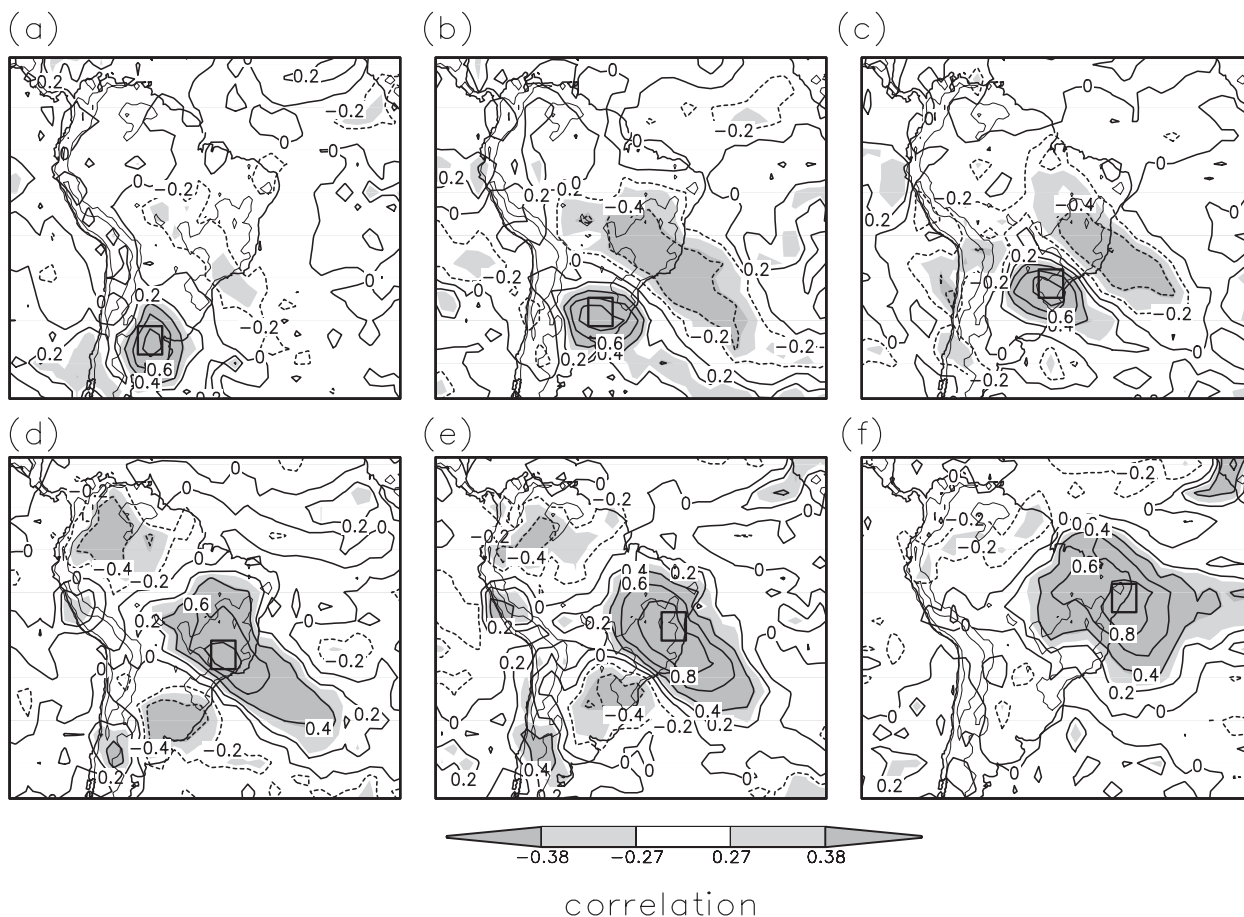


FIG. 2. Correlation of monthly precipitation with the precipitation over the reference area (shown as a solid-line rectangle in each panel) for January and February between 1979 and 2005. Absolute values of correlation coefficients more than 0.38 (between 0.38 and 0.28) are thick (thin) shaded for the 5% significance level, corresponding to 27 (between 27 and 54) independent samples (see text).

were set by the nudging process. SST data were obtained from the NOAA Optimal Interpolation version 2 monthly SST (OISST) analysis data with  $1^\circ \times 1^\circ$  (lat  $\times$  lon) resolution (Reynolds et al. 2002). Details on the numerical experiments are given in section 4.

### 3. Influence of the BP on the SACZ observed in the real atmosphere

In this section, the influence of the BP on the SACZ is examined by statistical analysis. The upper panels of Fig. 1 show the precipitation derived from the CMAP data and the low-level (850 hPa) wind and geopotential height derived from the NCEP–NCAR reanalysis averaged over 27 austral summers (January and February). The SACZ extends southeastward toward the South Atlantic across the Brazilian Plateau. The SACZ is a convergence zone between northerly flow in the western periphery of subtropical high over South Atlantic and northwesterly

flow from the Amazon basin. The latter is referred to as the South American low-level jet (SALLJ) when it is strong (Nogues-Paegle and Mo 1997; Marengo et al. 2004). A mesoscale cyclonic circulation is found over the western part of the BP. This helps to intensify the low-level convergence along the SACZ (Grimm et al. 2007). Hereafter the cyclonic circulation is referred to as the Brazilian Plateau cyclonic circulation (BPC).

The bottom panels of Fig. 1 show composites for cases where the monthly averaged precipitation over a reference area shown in the figure exceeded  $8 \text{ mm day}^{-1}$  (top 30% of the monthly precipitation). The precipitation was stronger over the BP, as expected, but also along the SACZ over the South Atlantic. The BPC and associated trough in the southwestern side of the SACZ were stronger than in the climatology (cf. upper panels of Fig. 1).

The SACZ shifts in a southwest–northeast direction along the southeastern coast of South America around

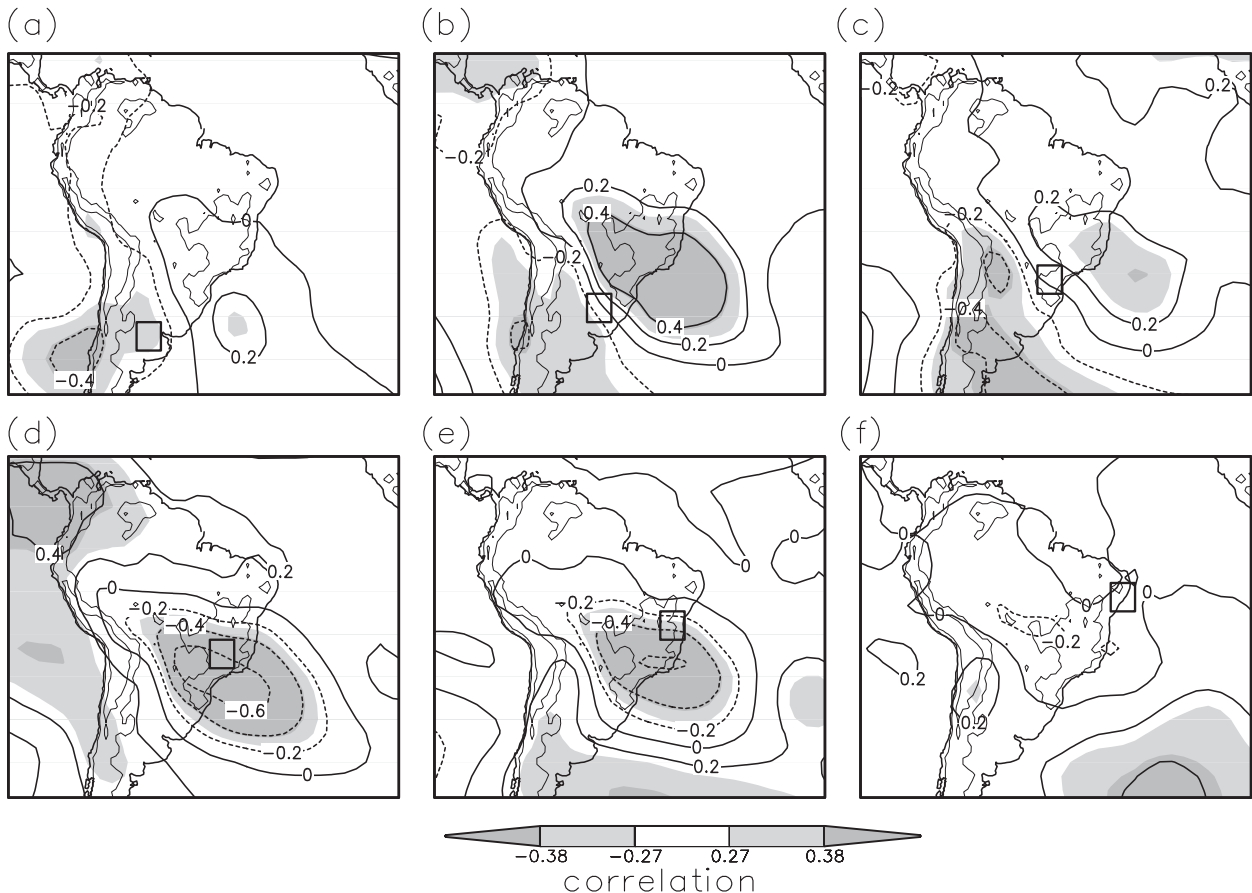


FIG. 3. As in Fig. 2, but for correlation of monthly averaged geopotential height at 850 hPa with the precipitation over the reference areas.

the climatological position of the SACZ, extending past the BP. To specify the preferred position of the SACZ and examine its relationship to the low-level circulation, we show the precipitation-to-precipitation correlation (Fig. 2) and the precipitation correlation to 850-hPa geopotential height (Fig. 3) for several reference areas of precipitation along the Atlantic coast. Correlations were calculated from 54 samples of monthly averages. We show two different 5% significance levels for the correlation coefficient: one based on the assumption that January and February data are independent, corresponding to 54 independent samples and a significance level 0.28, and the other based on the extreme assumption that successive January and February data are perfectly dependent, corresponding to a sample size half of the original, namely 27, and significance level 0.38. Considering the dependency in precipitation between the two successive months, an adequate significant level would be between 0.28 and 0.38. Positive precipitation-precipitation correlation extended southeastward over the South Atlantic for each reference area. The extension of this positive correlation toward the South Atlantic was

largest for the reference area over the BP (Figs. 2d,e). Figure 3 shows that there was negative correlation between precipitation and 850-hPa height to the southwest of the reference areas (Figs. 3b–e). The correlation was largest in the reference areas over the BP (Figs. 3d,e), indicating that the BPC was most intensified when the SACZ was located in its climatological position that passed through the BP. This result is consistent with previous remarks on the relationship between the intensification of the BPC and precipitation over the BP (Grimm et al. 2007; Grimm and Zilli 2009). Precipitation over southern Brazil, Uruguay, and Argentina also accompanied a negative height anomaly to the southwest (Figs. 3b,c).

The BPC does not form over the BP but is shifted southwestward (Fig. 1). To examine the reason for this, we perform a vorticity budget analysis using monthly averaged reanalysis data for the January 1985 case when the SACZ was active and persistent. When we neglect the vertical advection and twisting terms, which are relatively small, the vorticity equation in equilibrium is approximated as

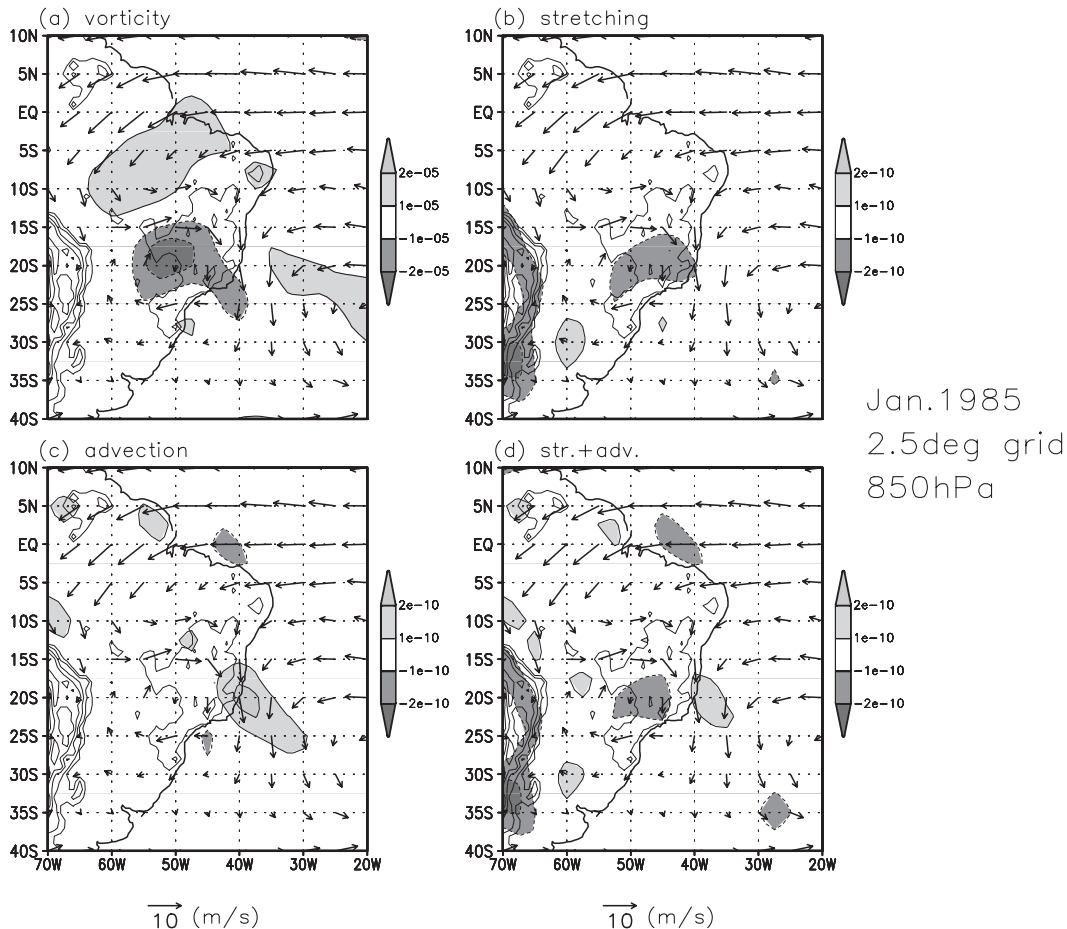


FIG. 4. Vorticity budget for the January 1985 case: (a) monthly averaged relative vorticity at 850 hPa, (b) generation of relative vorticity by the stretching process, (c) planetary vorticity advection, and (d) summation of vorticity generation by stretching and vorticity advection.

$$\mathbf{v} \cdot \nabla(f + \xi) = -(f + \xi)\nabla \cdot \mathbf{v} - \varepsilon\xi, \quad (1)$$

where  $\mathbf{v} = (u, v)$ ,  $f$ ,  $\xi$ , and  $\varepsilon$  are the horizontal velocity, Coriolis parameter, relative vorticity, and coefficient of Rayleigh friction, respectively. In the subtropics, where  $f$  is much larger than in the tropics, low-level convergence induced by the upward motion and maintained by the atmospheric heating forms a strong vorticity source. When the strength of the vorticity source exceeds the viscous vorticity dissipation, the source should be canceled by advection of absolute vorticity. In the lower troposphere, where mean westerlies are weak, this balance may approach the Sverdrup balance:

$$\beta\mathbf{v} = -f\nabla \cdot \mathbf{v}, \quad (2)$$

where  $\beta = \partial f / \partial y$ . A poleward wind, which advects relatively low absolute vorticity air, is required in the heating area. This poleward wind is maintained in the eastern part of cyclonic vorticity that appears to the west

of the BP center around 20°S, 45°–55°W (Fig. 4a). Generation of cyclonic vorticity by stretching appears over the BP around 20°S, 40°–55°W to the east of the vorticity center (Fig. 4b). This generation is partly canceled by advection of planetary vorticity, which dominates over the eastern part of the BP (Fig. 4c). As a result, the eastern part of vorticity generation is canceled, and the region of cyclonic vorticity generation is located over the western part of the BP (Fig. 4d).

The vorticity analysis indicated that rainfall areas formed a cyclonic circulation to the west, while the correlation analysis showed that a negative height correlation appeared to the southwest and extended southeast of the precipitation reference area in every panel of Fig. 3 (especially in Figs. 3b–e). This probably occurred because the precipitation was not confined to the reference area but extended southeastward (cf. Fig. 2). The negative height anomaly was maintained to the west of the precipitation zone but extended southeastward in parallel

TABLE 1. Conditions for the Control run.

Period	January 1985 (31 days) and December 1995 (31 days)
Spin up time	10 days
Initial condition	NCEP–NCAR reanalysis ( $2.5^\circ \times 2.5^\circ$ grid)
Boundary condition	NCEP–NCAR reanalysis (6 hourly, $2.5^\circ \times 2.5^\circ$ grid)
Grid number	$400 \times 350$
Vertical layer	30 ( $z^*$ coordinate): interval is 80 m at the bottom and increases with a stretch ratio of 1.2
Grid interval	25 km
Time step interval	30 s
SST	NOAA OISST v.2
Convective parameterization	Arakawa and Schubert (Numaguti et al. 1997)
Radiation scheme	Nakajima (Nakajima et al. 2000)

with the precipitation zone. This is consistent with the results of the vorticity budget analysis that showed that atmospheric heating formed cyclonic vorticity to the west. Negative correlation was maximum when the reference area was at the BP, and the precipitation zone showed the largest extent toward the ocean (Figs. 2d and 3d). This suggests another link between the BP and SACZ; that is, cyclonic circulation induced moisture flow to the BP, which intensified the precipitation by topographically induced convergence (Grimm et al. 2007; Grimm and Zilli 2009).

#### 4. Design of numerical experiments using TERC-RAMS

The statistical analysis in section 3 indicates that the SACZ intensified when it passed over the Brazilian Plateau. When the SACZ was located over the BP, the BPC appeared to the southwest of the SACZ and intensified low-level convergence along it. To understand why the BP is the favored location for the SACZ and the BPC is enhanced there, we performed several sensitivity experiments using TERC-RAMS. Details of the Control run are shown in Table 1. We selected two months, January 1985 and December 1995, as study periods when the SACZ was active and located in the climatic position. Figure 5 shows the CMAP precipitation, 850-hPa wind, and geopotential height averaged over these periods. The SACZ was significant and located in the climatic position (cf. Fig. 1) passing through the BP. The BPC appeared to the west of the BP and intensified the low-level convergence along the SACZ. These monthly averaged fields around the SACZ are similar to those of the climatology, although the BPC was stronger than that in the climatology for January 1985 (cf. Fig. 1).

Conditions for sensitivity experiments are shown in Table 2. Figure 6 shows the topography around the BP adopted in each experiment. A dashed rectangle in each panel represents the reference area of precipitation over the BP shown in Table 3. To represent the complex topography over the BP, the horizontal resolution was 25 km in the “Control” run. We also performed a

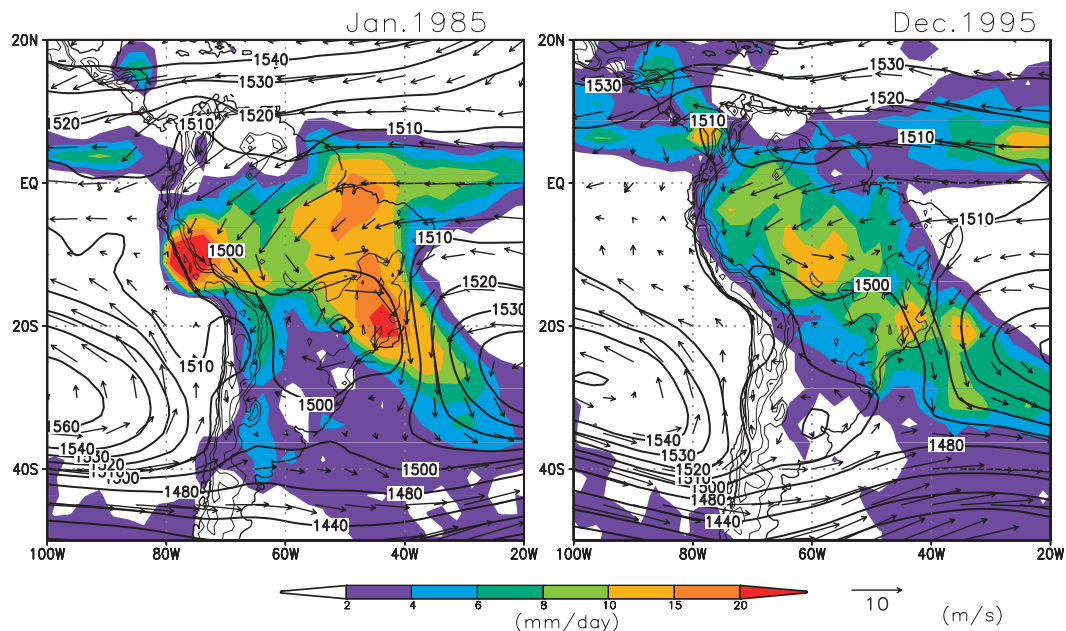


FIG. 5. Monthly averaged CMAP precipitation ( $\text{mm day}^{-1}$ ) and 850-hPa wind ( $\text{m s}^{-1}$ ) and geopotential height (m) averaged in January 1985 and December 1995.

TABLE 2. Conditions of sensitivity experiments.

Run	Conditions
Control	
Smoothed BP	Topography around the BP is smoothed
Removed BP	Topography around the BP is reduced to 0%
Low Resolution	Grid interval is 150 km
Stop Rain	Rainfall is artificially stopped around the BP

“Smoothed BP” run and a “Removed BP” run. In the former, topography around the BP was smoothed, similar to in the “Low-Resolution” run that had 150-km resolution, to examine the influence of complex topography

of the BP. In the latter, the altitude was set to 0 m around the BP to examine the influence of the BP as a mass of mountains. The modification of topography was done within a solid-line rectangle in each panel for these runs (Figs. 6a,c,d). Topographic modification was applied gradually near the boundary to avoid steep slopes that could cause unnatural local circulation. The Low-Resolution run was performed to examine the dependency of model resolution, which may change precipitation not only through the changed representation of topography, but also by deferring atmospheric processes in the model, such as cumulus parameterization. The “Stop Rain” run

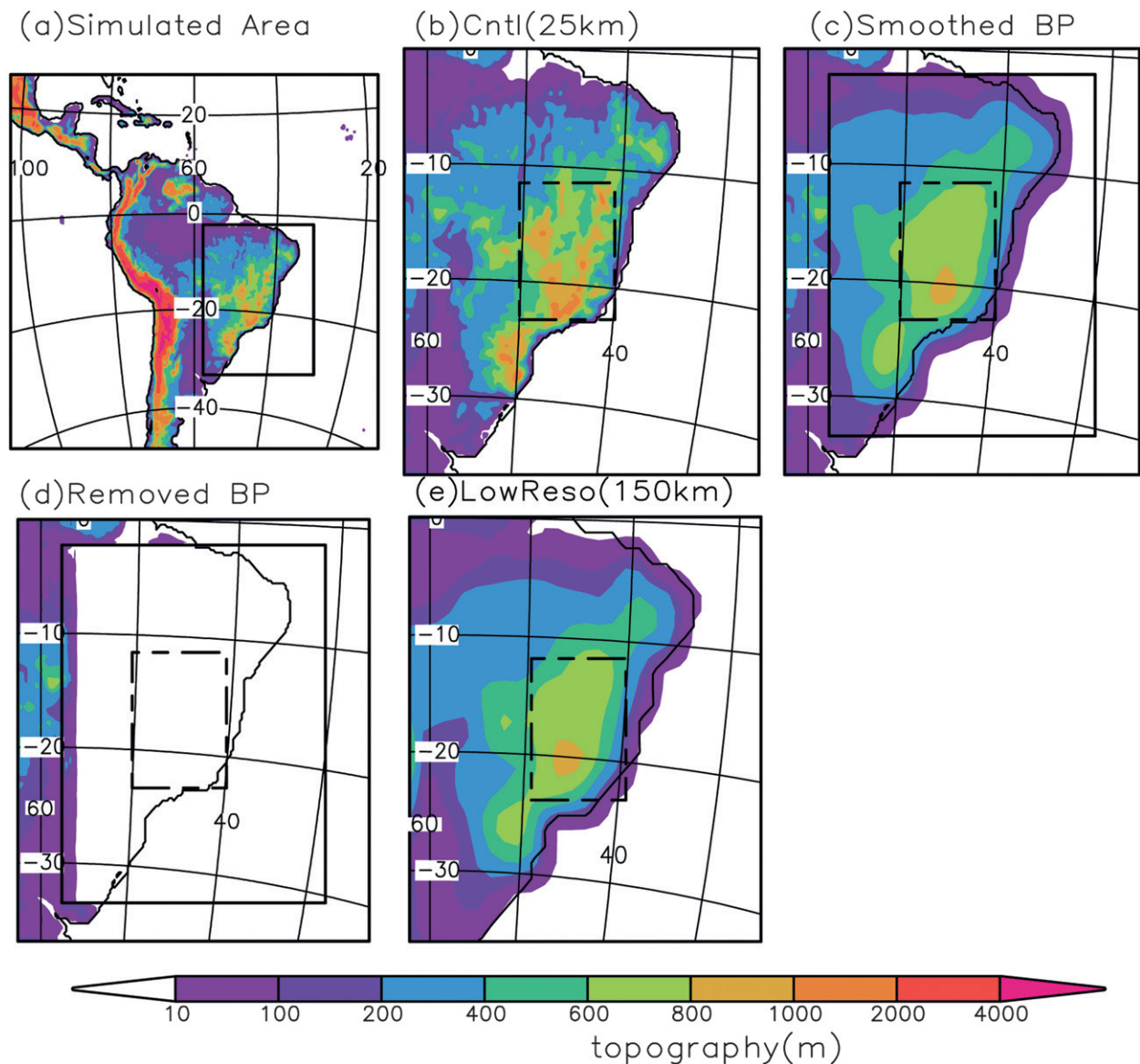


FIG. 6. Domain of (a) the simulated area and (b)–(e) topography represented in each run. The solid-line rectangles in (a), (c), and (d) represent the area in which topography was modified in the Removed BP and Smoothed BP runs. Dashed-line rectangles in (b)–(e) indicate the reference area for precipitation over the BP.

TABLE 3. Precipitation ( $\text{mm day}^{-1}$ ) averaged over the Brazilian Plateau in each run.

Run	January 1985	December 1995
Control	7.16	5.10
Smoothed BP	6.71	4.41
Removed BP	6.12	3.78
Low Resolution	1.76	2.38
Stop Rain	0.04	0.02

was performed to examine the roles of latent heating due to precipitation over the BP. In this run, rainfall around the BP, along with accompanying latent heat, was stopped artificially by absorbing the moisture at all levels in the model around the BP. This treatment has the advantage of not forming unnaturally strong precipitation around the rain-stopped area due to excess moisture that was not consumed there. Extra forcing by dry processes such as midlatitude wave trains was retained despite the moisture absorption. The disadvantage was that moisture absorption reduced precipitation not only over the area but also downstream due to dry air advection.

The results of the Control run for each month, in Fig. 7, show monthly averaged precipitation and 850-hPa wind and geopotential height. Most characteristics of the SACZ were well simulated, including its location, width, and horizontal extension of precipitation along

the SACZ, although the simulated precipitation over South America including the BP was weaker than the observed precipitation in both cases (cf. Fig. 5). Moreover, in 1985 case, the peak of precipitation shifted westward in the Control run. The cyclonic circulation corresponding to the BPC was simulated in the 1985 case, although it was weaker than in the real atmosphere and shifted westward. The cyclonic circulation was very weak in the 1995 case (cf. Fig. 5).

## 5. Results of sensitivity experiments

Table 3 shows precipitation over the BP in each experiment for the two cases. The precipitation was averaged over the reference area, as shown in Fig. 6 by the dashed rectangles. Precipitation over the BP was suppressed in experiments in which the BP was removed or the complex BP topography was smoothed out (Table 3). The precipitation decrease was greater in the Removed BP run than in the Smoothed BP run.

Figure 8 shows the monthly mean distribution of precipitation, 850-hPa height, and 850-hPa wind in each run for the 1985 case. In this figure, the cyclonic circulation corresponding to the BPC was represented in the Control run. In the Smoothed BP and Removed BP runs, precipitation was suppressed over the BP compared

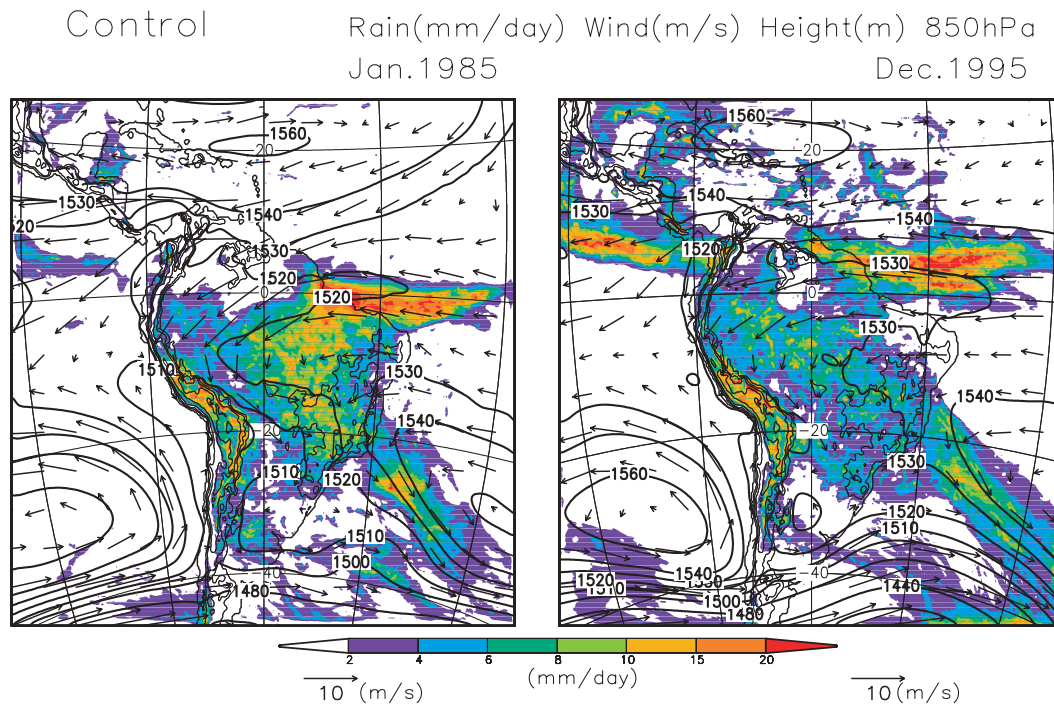


FIG. 7. Monthly averaged precipitation (color) and 850-hPa wind (vectors) and geopotential height (thick contours) for the Control run in January 1985 and December 1995. Topography is shown by thin contours over land.

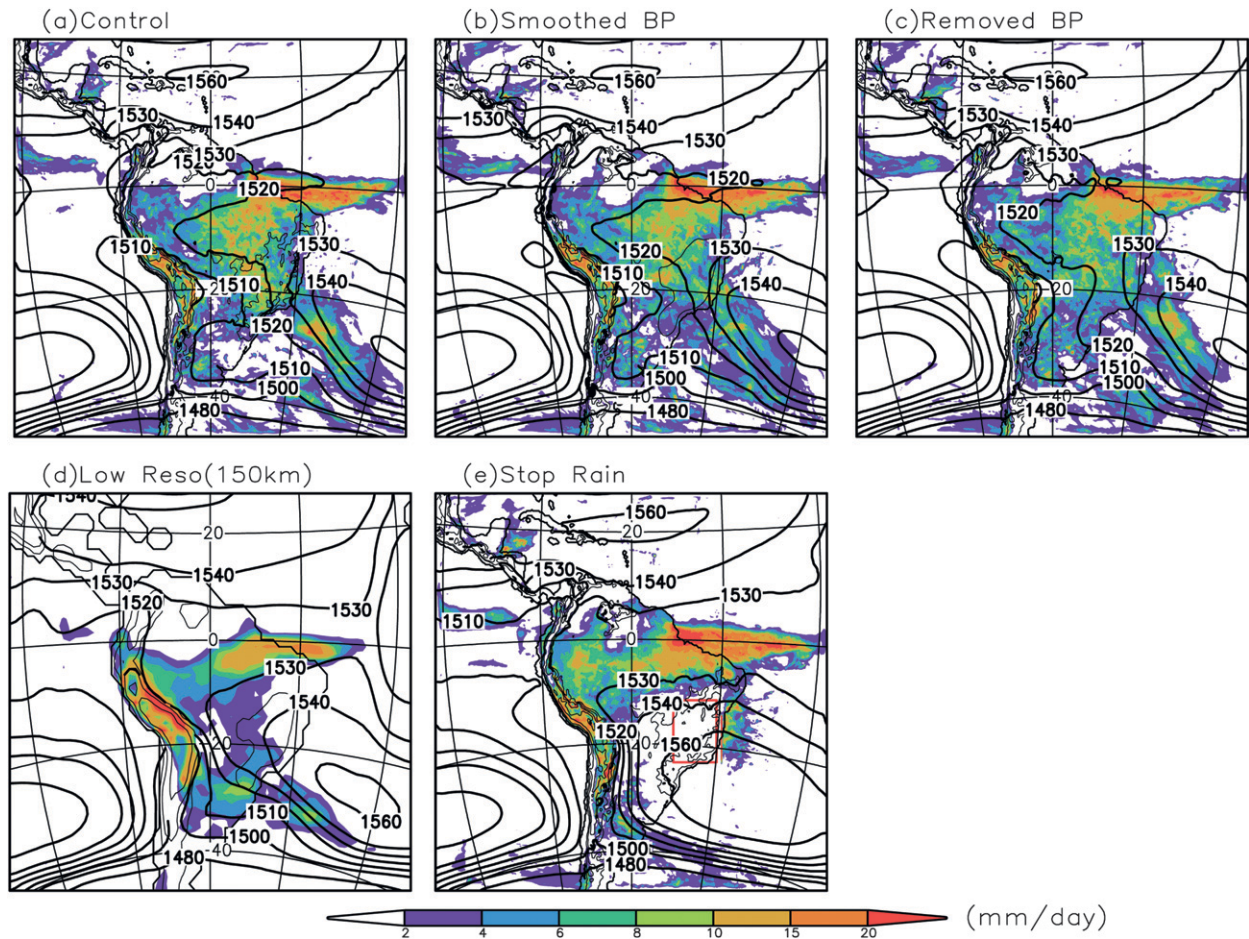


FIG. 8. Monthly averaged precipitation and 850-hPa geopotential height in each run in January 1985. (e) The red rectangle over southeastern Brazil shows the area where moisture was artificially absorbed.

to the Control run. Cyclonic circulation corresponding to the BPC was found but was weaker than in the Control run. In the Low Resolution run, precipitation around the BP was suppressed and the SACZ shifted southward, as found by Grimm et al. (2007) who reported that the SACZ shifted southward in their regional model when the BP was flattened. The BPC to the southwest of the BP disappeared. The ridge and accompanying anticyclonic circulation of the subtropical high over the South Atlantic crossed over the continent around 20°S. Easterlies from the South Atlantic flowed over the continent and turned southward at midlatitudes. In the Stop Rain run, precipitation ceased around the rectangle where the air was artificially dried and was also reduced downstream by dry air advection. The low-level circulation changed: the BPC to the southwest of the BP disappeared, and a ridge-accompanying easterly wind from the South Atlantic deeply invaded the continent. The SACZ-accompanied low-level convergence shifted far southward to the midlatitudes near 40°S, as also demonstrated by Grimm

et al. (2007). In the 1995 case, the BPC was not clearly represented in the Control run (Fig. 7). However, we found a similar tendency in precipitation over the BP and a southward shift of the SACZ.

Figure 9 shows the anomaly of precipitation, 850-hPa wind, and 850-hPa geopotential height from the Control run for each run of the two cases. For the Low Resolution run, the anomaly was calculated by referencing the results of the Control run after interpolating to the same grid used in the Low Resolution run. A precipitation decrease over the BP was observed in the Smoothed BP, Removed BP, and Low Resolution runs in both cases. A negative anomaly of precipitation extended southeastward over the South Atlantic, along with an anomalous ridge and anticyclonic circulation. The negative anomaly accompanied a positive anomaly of precipitation to the south, indicating a southward shift of the SACZ in these experiments. In the 1985 case, a localized anticyclonic anomaly was found to the southwest of the BP (27°S, 53°W) in the Smoothed BP and Removed BP runs.

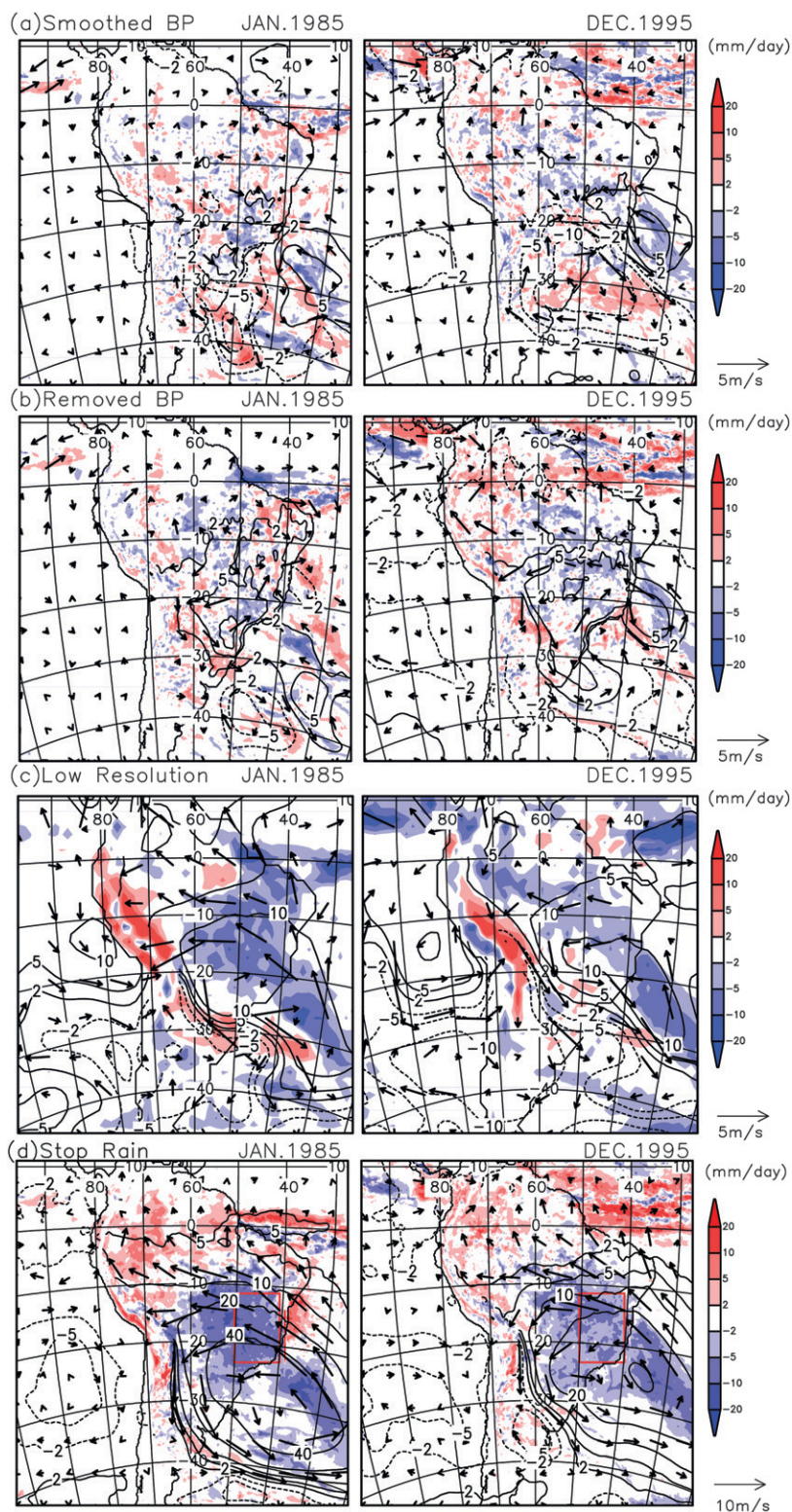


FIG. 9. Monthly averaged anomaly (i.e., difference from the Control run) in precipitation (color shading between deep red and dark purple), 850-hPa wind (vectors), and 850-hPa geopotential height (contours) for the (a) Smoothed BP, (b) Removed BP, (c) Low Resolution, and (d) Stop Rain runs in the two cases. The red rectangle over southeastern Brazil in (d) shows the area where moisture was artificially absorbed.

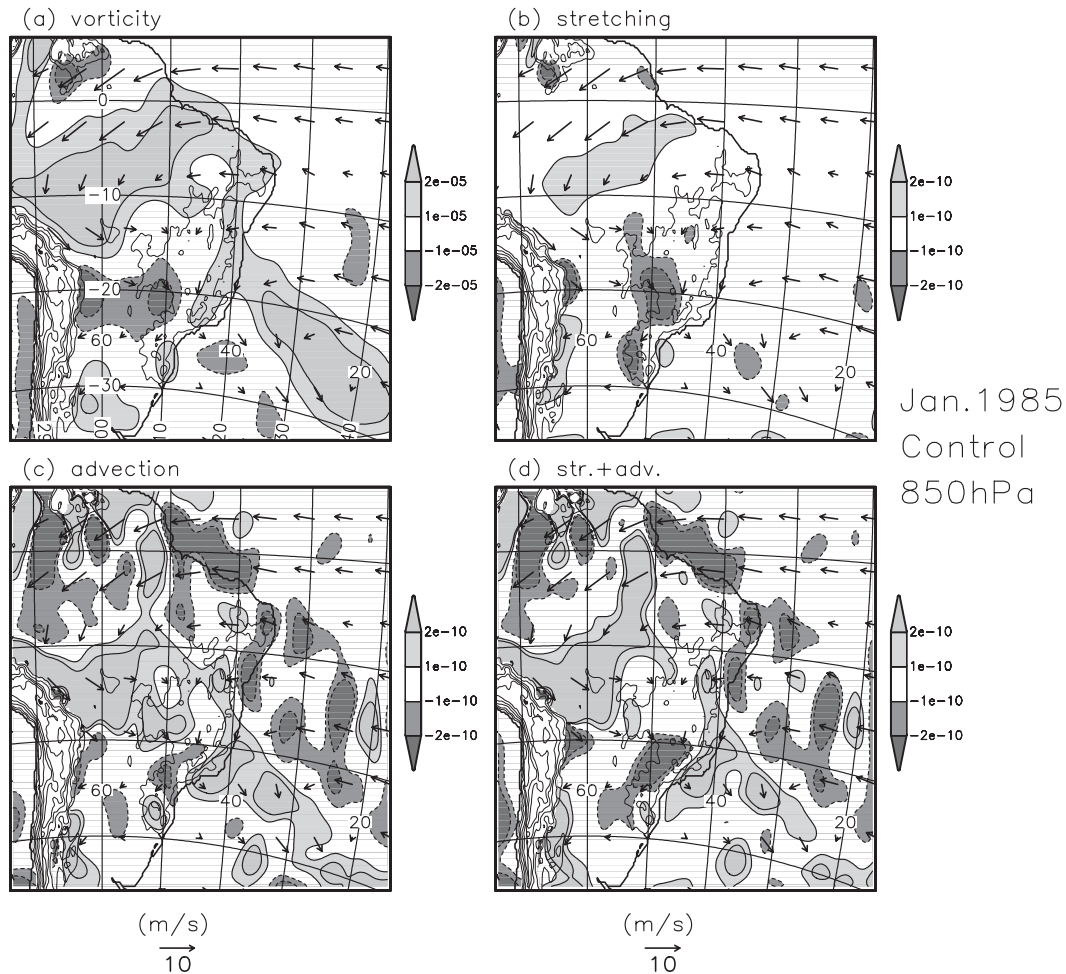


FIG. 10. As in Fig. 4, but for the Control run.

The anomaly was also found as a bulge ( $27^{\circ}\text{S}$ ,  $53^{\circ}\text{W}$ ) in the Low Resolution run. This corresponded to a weakening of the BPC. Such a localized anomaly was not found in the 1995 case, probably due to the weak representation of BPC in the Control run (Fig. 7). The negative anomaly of precipitation along the SACZ and the anticyclonic circulation were much stronger in the Stop Rain run than in the BP modification experiments, suggesting that the circulation maintaining the SACZ was closely related to the precipitation over the BP because the circulation changed significantly when the precipitation over the BP was artificially stopped. The SACZ was strongest in experiments when fine topography was represented in the model.

## 6. Vorticity budget analysis in numerical experiments

In the Control run, as in the real atmosphere, the BPC did not form over the BP but shifted to the west. We

performed a vorticity budget analysis for the Control run and the Stop Rain run. The results for the Control run were similar to the reanalysis data (Fig. 4). Cyclonic vorticity appeared to the west of the BP center around  $20^{\circ}\text{S}$ ,  $45^{\circ}\text{--}55^{\circ}\text{W}$  (Fig. 10a). Cyclonic vorticity was generated by stretching over the BP around  $20^{\circ}\text{S}$ ,  $50^{\circ}\text{W}$  to the east of the vorticity center (Fig. 10b). This generation was partly canceled by advection of planetary vorticity over the eastern part of the BP (Fig. 10c). As a result, cyclonic vorticity was maintained only over the western part of the BP (Fig. 10d). Figure 11 shows the results of the Stop Rain run. Here, generation of vorticity by convergence disappeared around the BP, and the cyclonic circulation was no longer maintained. This indicates that the Brazilian Plateau cyclonic circulation can be maintained by the updraft associated with the latent heat of precipitation over the BP, and the precipitation may have been intensified by the topographical updraft and local circulation induced by complex topography.

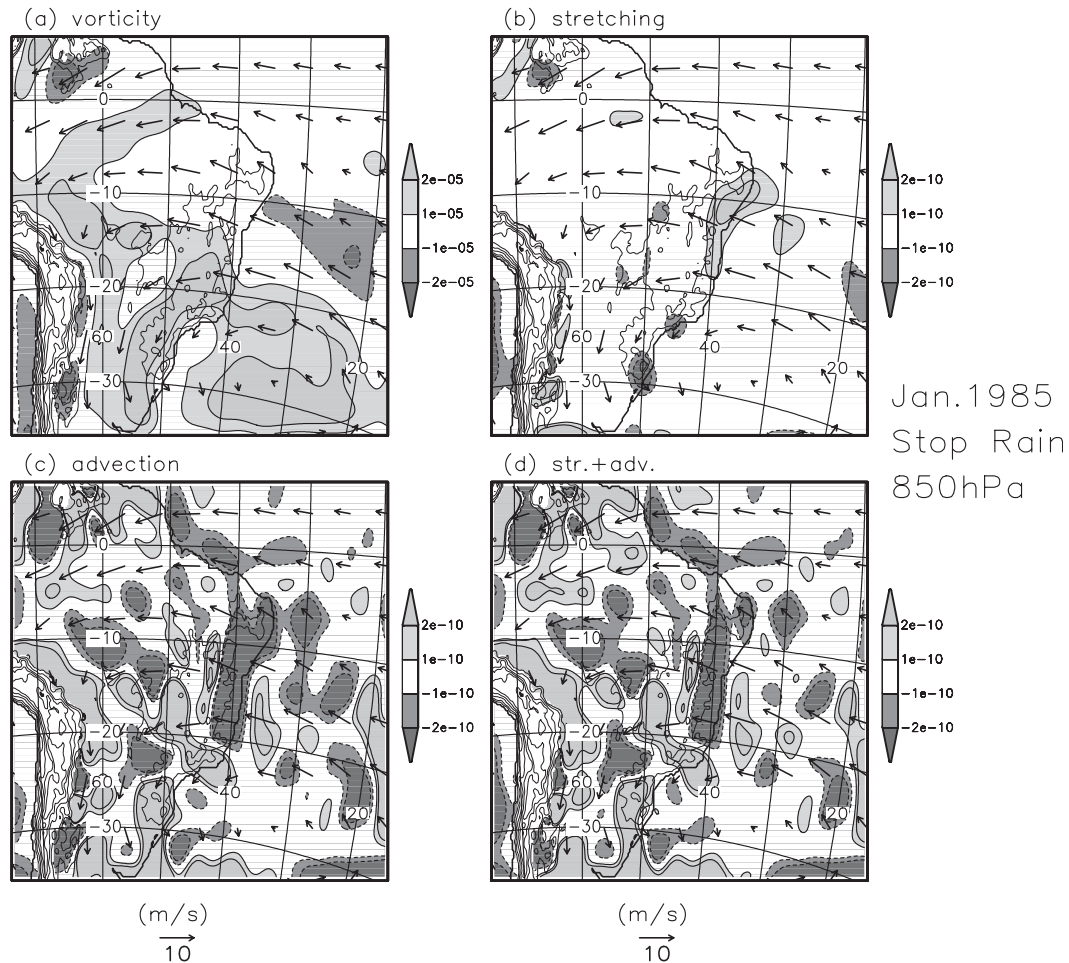


FIG. 11. As in Fig. 4, but for the Stop Rain run.

## 7. Summary and discussion

We studied mechanisms for maintaining the SACZ, emphasizing the role of the BP. The results of our statistical study indicated that the SACZ was most intensified when it passed over the BP. Precipitation over the BP formed a low-level cyclonic circulation to the southwest of the BP, which intensified low-level convergence along the SACZ over southeastern Brazil.

Several sensitivity experiments were performed for two cases when the SACZ was strong and located in the climatic position on monthly bases. The Stop Rain run clearly showed that precipitation over the BP maintained the low-level cyclonic circulation corresponding to the BPC to the southwest of the BP and the convergence along the SACZ over the continent. Without the BPC, a subtropical ridge invaded the BP and the precipitation zone shifted southward from the climatic position of the SACZ. There were some differences between the cases in sensitivity experiments where the BP topography was

removed or smoothed, or the resolution was reduced. However, we found the following general features: (i) the precipitation over the BP was reduced, (ii) the BPC was weakened in cases where the BPC was represented in the Control run, and (iii) the precipitation zone SACZ shifted southward. The results of the sensitivity experiments indicated that removing the topography or not representing it properly reduced the precipitation over the BP and tended to shift the SACZ southward, as found by Grimm et al. (2007). Our results also support the idea that the BP has an anchoring effect on the seesaw pattern related to the SACZ, as suggested by Grimm et al. (2007), because the topography of the BP intensifies precipitation there. Moreover, our results support the CISK mechanism between precipitation over the BP and the development of the Brazilian Plateau cyclonic circulation. This intensifies convergence over the BP, as proposed by Grimm et al. (2007). Our experiments involved only two cases. Statistical study based on sensitivity experiments for many cases is desirable in the future.

*Acknowledgments.* Discussions with Dr. K. Ninomiya, Dr. N. Sato, and Prof. A. Grimm were useful for this study. Comments from anonymous reviewers were very constructive and useful and improved this study. This study was supported by a Grant-in-Aid for Scientific Research from Japan's Ministry of Education, Culture, Sports, Science and Technology, Projects 17540407 and 21540449.

## REFERENCES

- Carvalho, L. M. V., C. Jones, and B. Liebmann, 2004: The South Atlantic convergence zone: Intensity, form, persistence, and relationships with intraseasonal to interannual activity and extreme rainfall. *J. Climate*, **17**, 88–108.
- , A. E. Silva, C. Jones, B. Liebmann, P. L. Silva Dias, and H. R. Rocha, 2010: Moisture transport and intraseasonal variability in the South America monsoon system. *Climate Dyn.*, **36**, 1865–1880, doi:10.1007/s00382-010-0806-2.
- Cook, K. H., 2000: The South Indian convergence zone and interannual rainfall variability over southern Africa. *J. Climate*, **13**, 3789–3804.
- Diaz, A., and P. Aceituno, 2003: Atmospheric circulation anomalies during episodes of enhanced and reduced convective cloudiness over Uruguay. *J. Climate*, **16**, 3171–3185.
- Ding, Y., 1992: Summer monsoon rainfall in China. *J. Meteor. Soc. Japan*, **70**, 373–396.
- Figueroa, S. N., P. Satyamurty, and P. L. Silva Dias, 1995: Simulations of the summer circulation over the South American region with an eta coordinate model. *J. Atmos. Sci.*, **52**, 1573–1584.
- Grimm, A. M., and M. T. Zilli, 2009: Interannual variability and seasonal evolution of summer monsoon rainfall in South America. *J. Climate*, **22**, 2257–2275.
- , C. S. Vera, and C. R. Mechoso, 2005: The South American monsoon system. *The Global Monsoon System: Research and Forecast*, C.-P. Chang, B. Wang, and N.-C. G. Lau, Eds., WMO/TD 1266-TMRP 70, 219–238.
- , J. S. Pal, and F. Giorgi, 2007: Connection between spring conditions and peak summer monsoon rainfall in South America: Role of soil moisture, surface temperature, and topography in eastern Brazil. *J. Climate*, **20**, 5929–5945.
- Kodama, Y.-M., 1992: Large-scale common features of subtropical precipitation zones (the baiu frontal zone, the SPCZ and the SACZ). Part I: Characteristics of subtropical frontal zones. *J. Meteor. Soc. Japan*, **70**, 813–836.
- , 1993: Large-scale common features of subtropical convergence zones (the baiu frontal zone, the SPCZ and the SACZ). Part II: Conditions of the circulations for generating the STCZs. *J. Meteor. Soc. Japan*, **71**, 581–610.
- , 1999: Roles of the atmospheric heat sources in maintaining the subtropical convergence zones: An aquaplanet GCM study. *J. Atmos. Sci.*, **56**, 4032–4049.
- Lenters, J. D., and K. H. Cook, 1995: Simulation and diagnosis of the regional summertime precipitation climatology of South America. *J. Climate*, **8**, 2988–3005.
- Liebmann, B., and C. Smith, 1996: Description of a complete (interpolated) outgoing longwave radiation dataset. *Bull. Amer. Meteor. Soc.*, **77**, 1275–1277.
- , G. Kiladis, J. Marengo, T. Ambrizzi, and J. D. Glick, 1999: Submonthly convective variability over South America and the South Atlantic convergence zone. *J. Climate*, **12**, 1877–1891.
- Marengo, J. A., W. R. Soares, C. Saulo, and M. Nicolini, 2004: Climatology of the low-level jet east of the Andes as derived from the NCEP–NCAR reanalyses: Characteristics and temporal variability. *J. Climate*, **17**, 2261–2280.
- Murakami, T., L.-X. Chen, and A. Xie, 1986: Relationship among seasonal cycles, low-frequency oscillation, and transient disturbances as revealed from outgoing longwave radiation data. *Mon. Wea. Rev.*, **114**, 1456–1465.
- Muza, M.-N., L. M. V. Carvalho, C. Jones, and B. Liebmann, 2009: Intraseasonal and interannual variability of extreme dry and wet events over southeastern South America and the subtropical Atlantic during austral summer. *J. Climate*, **22**, 1682–1699.
- Nakajima, T., M. Tsukamoto, Y. Tsushima, A. Numaguti, and T. Kimura, 2000: Modeling of the radiative process in an atmospheric general circulation model. *Appl. Opt.*, **39**, 4869–4878.
- Ninomiya, K., 2007: Similarity and difference between the South Atlantic convergence zone and the Baiu frontal zone simulated by an AGCM. *J. Meteor. Soc. Japan*, **85**, 277–299.
- , 2008: Similarities and differences among the South Indian Ocean convergence zone, North American convergence zone, and other subtropical convergence zones simulated using an AGCM. *J. Meteor. Soc. Japan*, **86**, 141–165.
- Nogues-Paegle, J., and K.-C. Mo, 1997: Alternating wet and dry conditions over South America during summer. *Mon. Wea. Rev.*, **125**, 279–291.
- , and —, 2002: Linkages between summer rainfall variability over South America and sea surface temperature anomalies. *J. Climate*, **15**, 1389–1407.
- Numaguti, A., M. Takahashi, T. Nakajima, and A. Sumi, 1997: Description of CCSR/NIES Atmospheric General Circulation Model. CGER's Supercomputer Monograph Rep. 3, Center for Global Environmental Research, National Institute for Environmental Studies, 1–48.
- Pielke, R. A., and Coauthors, 1992: A comprehensive meteorological modeling system—RAMS. *Meteor. Atmos. Phys.*, **49**, 69–91.
- Reynolds, R. W., N. A. Rayner, T. M. Smith, D. C. Stokes, and W. Wang, 2002: An improved in situ and satellite SST analysis for climate. *J. Climate*, **15**, 1609–1625.
- Sato, T., and F. Kimura, 2003: A two-dimensional numerical study on diurnal cycle of mountain lee precipitation. *J. Atmos. Sci.*, **60**, 1992–2003.
- Streten, N. A., 1975: Satellite-derived inferences to some characteristics of the South Pacific atmospheric circulation associated with the Niño event of 1972–73. *Mon. Wea. Rev.*, **103**, 989–995.
- Vera, C., and Coauthors, 2006: Toward a unified view of the American monsoon systems. *J. Climate*, **19**, 4977–5000.
- Xie, P., and P. A. Arkin, 1997: Global precipitation: A 17-year monthly analysis based on gauge observations, satellite estimates, and numerical model outputs. *Bull. Amer. Meteor. Soc.*, **78**, 2539–2558.
- Zhou, J., and K. M. Lau, 1998: Does a monsoon climate exist over South America? *J. Climate*, **11**, 1020–1040.